

Relaxation of spin-glass magnetization in $\text{Cd}_{1-x}\text{Mn}_x\text{Te}$ diluted magnetic semiconductors

M. Smith, A. Dissanayake, and H. X. Jiang

Department of Physics, Kansas State University, Manhattan, Kansas 66506-2601

(Received 7 September 1993)

Relaxation of thermal-remanent magnetization and isothermal remanent magnetization of spin glass in $\text{Cd}_{1-x}\text{Mn}_x\text{Te}$ diluted magnetic semiconductors have been studied at different conditions. Magnetization relaxation can be described by a power-law decay, $M(t) = M_0 t^{-\alpha}$ ($t > t_0$ and $t_0 = 2$ s) with small values of α or a logarithmic decay $M(t) = M_0(1 - \alpha \ln t)$ ($t > t_0$ and $t_0 = 2$ s). Temperature and applied magnetic-field dependencies of the decay parameter α have been measured. The above-band-gap photoexcitation has been used to generate free carriers (electrons and holes) in the sample and their effects on the spin-spin interaction of Mn ions have been studied. The dependence of the power-law decay parameter α on excitation light intensity has also been measured. It is found that α is proportional to the photogenerated carrier concentration. Furthermore, aging effects in the spin-glass state have also been studied by varying the time duration of the applied magnetic field. The transient responses of magnetization in the spin-glass state upon applying a magnetic field in the dark and under illumination have been measured and are found to follow a power-law time dependence, $M(t) = M_0 + M_1 t^\beta$. Temperature and the applied magnetic-field dependencies of the transient parameter β have been measured. A mechanism, involving an increased spin domain size under light illumination via free-carrier-Mn spin interaction, can explain our results very well.

I. INTRODUCTION

Diluted magnetic semiconductors (DMS's) have been a group of materials attracting a great deal of attention for many years because of their unique properties for understanding much fundamental physics as well as promising practical applications.^{1,2} DMS's are semiconductors formed by replacing a fraction of the cations in a range of compound semiconductors with transition-metal ions. Some examples of the DMS are $\text{Cd}_{1-x}\text{Mn}_x\text{Te}$, $\text{Pb}_{1-x}\text{Mn}_x\text{Te}$, and $\text{Zn}_{1-x}\text{Fe}_x\text{Se}$. These can be expressed generally as $A_{1-x}M_xB$. Here x indicates the fraction of the nonmagnetic cations (A) of the compound semiconductors (AB) which is randomly replaced by magnetic $3d$ or $4f$ ions (M). Formation of the DMS can also be described as alloying an ordinary semiconductor AB with a magnetic semiconductor MB in the desired proportion. The magnetic behavior of different kinds of DMS shows many common characteristics, which can be understood on the basis of a random array of localized magnetic moments coupled by isotropic antiferromagnetic interaction.³ Many aspects of this interaction between magnetic ions are still under investigation.

DMS's also have many potential applications including infrared detectors,^{4,5} electroluminescent devices,⁶ and tunable Raman spin-flip lasers.⁷ Their fundamental semiconducting properties such as the energy band gap, carrier effective mass, mobility, etc. can be varied under control of the molar composition as in nonmagnetic semiconductor alloys. DMS device possibilities can be grouped into three classes.⁸ The first depends only on the semiconductor band gap or other composition-dependent properties. The second class of device utilizes optical transitions of the Mn^{2+} ion, such as electroluminescent devices. The third class of device is based on the $sp-d$ ex-

change interaction.

One of the interesting and important subjects in the DMS is the spin-glass (SG) state at low temperatures. It is well established in DMS's that there exists a paramagnetic SG transition at low temperatures due to the randomness of the magnetic ion distribution and spin-spin interactions. The transition temperature or freezing temperature T_f depends on magnetic ion composition,^{9,10} magnetic field,¹¹ and the history of the system. T_f has been calculated by a short-range mechanism, the main contribution of which comes from the antiferromagnetic interaction between nearest neighbors¹² or second or third neighbors,¹³ which is consistent with experimental results. Although some work previously has been devoted to study SG dynamics in the DMS,¹⁴⁻¹⁷ the understanding of the dynamic process of SG formation and transformation, as well as the relaxation in the SG state, are still far from complete.

In this paper, we report studies of the relaxation and transient response of thermal-remanent magnetization (TRM) and isothermal remanent magnetization (IRM) of $\text{Cd}_{1-x}\text{Mn}_x\text{Te}$ in the SG state at different temperatures and magnetic fields, and under light illumination with different excitation light intensities. Here relaxation refers to a process in which the magnetization decays slowly with time after the removal or reduction of an applied magnetic field. The transient response refers to the slow increasing of the magnetization upon applying a magnetic field. Both relaxation and transient responses can be observed in the SG state. Relaxation of magnetization is commonly studied to determine the magnetic properties of DMS's, while the transient response of magnetization is much less frequently studied in magnetic materials. However, the transient response is a very important technique in semiconductor research for study-

ing, for example, carrier excitation or conductivity under light excitation.

A power-law time dependence of TRM and IRM relaxation and transient response has been observed, and the decay parameter at different conditions has been determined. For relaxation, the decay parameters are very small and the kinetics can be described equally well by a logarithmic decay. The transient response and relaxation of magnetization are found to be correlated. The main results reported in this paper are investigations of the spin-spin interaction of magnetic ions in the SG state affected by photogenerated electrons and holes. We have measured TRM and IRM under light illumination at different conditions, and the results have been compared to those obtained in the dark. Comparison experiments on relaxation and transient responses of magnetization in the dark and under illumination have also been performed. The data have been analyzed in terms of a recently proposed percolation model for magnetic relaxation in random systems.

II. EXPERIMENT

The samples used for this study were $\text{Cd}_{1-x}\text{Mn}_x\text{Te}$ single crystals provided by Cleveland Crystal, Inc. Two different samples with Mn composition $x=0.26$ and 0.5 have been studied here. They were grown by the temperature gradient technique and are nominally undoped. However, photoluminescence measurements of a bound exciton transition indicated a low concentration of impurities in the samples. Results obtained for these two compositions ($x=0.26$ and 0.5) should represent general properties of the relaxation of spin-glass magnetization in $\text{Cd}_{1-x}\text{Mn}_x\text{Te}$ with different compositions. By comparing the results obtained for $x=0.26$ to those of $x=0.5$ samples, we can also learn the trend of the Mn composition dependence of the magnetization relaxation. The size of the samples was a few cubic millimeters. The magnetization was measured by a superconducting quantum interference device (SQUID) magnetometer (Quantum Design MPMS5). In order to study the effects of photoexcitation to the transient response and relaxation of TRM and IRM, a specially designed quartz optic fiber probe was used with the SQUID. The fiber optic probe was made of an optic fiber bundle with a diameter of about 2 mm. One end of the optic fiber probe was in the sample chamber with a distance of a few mm away from the sample, and the other end was outside the SQUID being used for light illumination. Different light sources have been used for light excitation, including a white desk lamp, Hg lamp, halogen lamp with filters, and He-Ne laser. Light intensity was controlled by a set of neutral density filters. The best response was obtained for the Hg lamp. Results reported here were obtained by using the Hg lamp as an excitation source except where indicated.

III. RESULTS AND DISCUSSIONS

A. Relaxation in the dark

We have measured the susceptibility of samples under field-cooled (FC) and zero-field-cooled (ZFC) conditions

to determine the freezing temperatures T_f of the SG state. For FC, the applied magnetic field during the cooling down was set at $B=1$ T. For each measurement, the system was always cooled down from room temperature to avoid hysteresis effects. For both FC and ZFC conditions, the susceptibility as a function of temperature was measured at a magnetic field of 100 Oe, starting from the lowest temperature. The data for two samples [$\text{Cd}_{0.74}\text{Mn}_{0.26}\text{Te}$ (circles) and $\text{Cd}_{0.5}\text{Mn}_{0.5}\text{Te}$ (squares)] are displayed in Fig. 1, which shows that T_f is about 4.2 ± 0.2 K for $\text{Cd}_{0.74}\text{Mn}_{0.26}\text{Te}$, and 19 ± 1 K for $\text{Cd}_{0.5}\text{Mn}_{0.5}\text{Te}$. In this paper, except in Fig. 2, we plot susceptibility M/B instead of magnetization M , since M depends linearly on B in the region of the measuring field. The reason for measuring the magnetization at a low field of 100 Oe instead of zero field is that experimentally we can obtain a better signal-to-noise ratio at a finite field. Figure 1 shows only experimental data in the region from 1.7 to 30 K for a clear presentation. These results are consistent with previous measurements.^{10,11,14,18} In this paper, we report only relaxation and transient responses of TRM and IRM in the SG state, or at temperatures below T_f . We did not observe any remanent magnetization or slow transient behavior for magnetization above T_f .

Figure 2 shows the comparison result of relaxation of TRM and IRM of $\text{Cd}_{0.74}\text{Mn}_{0.26}\text{Te}$ at $T=2.5$ K obtained

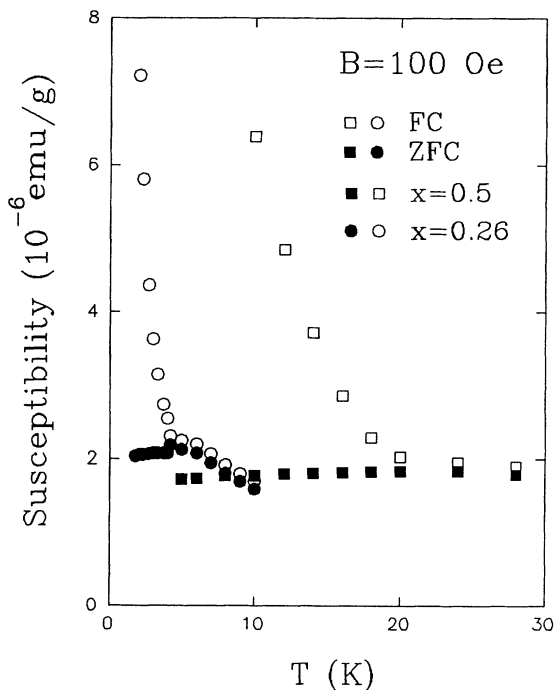


FIG. 1. The zero-field-cooled (ZFC $\bullet\bullet$ and $\blacksquare\blacksquare$) and field-cooled (FC $\circ\circ$ and $\square\square$) magnetic susceptibility of $\text{Cd}_{1-x}\text{Mn}_x\text{Te}$ measured at a magnetic field of 100 Oe for two samples, $x=0.26$ (\circ and \bullet) and 0.5 (\blacksquare and \square). The magnetic field applied during FC is 1 T for both samples. For each measurement, the system was always cooled down from room temperature to the lowest temperature, and the measurements were then started from the lowest temperature. The freezing temperature T_f obtained is $T_f=4.2\pm 0.2$ and 19 ± 1 K for $x=0.26$ and 0.5 , respectively.

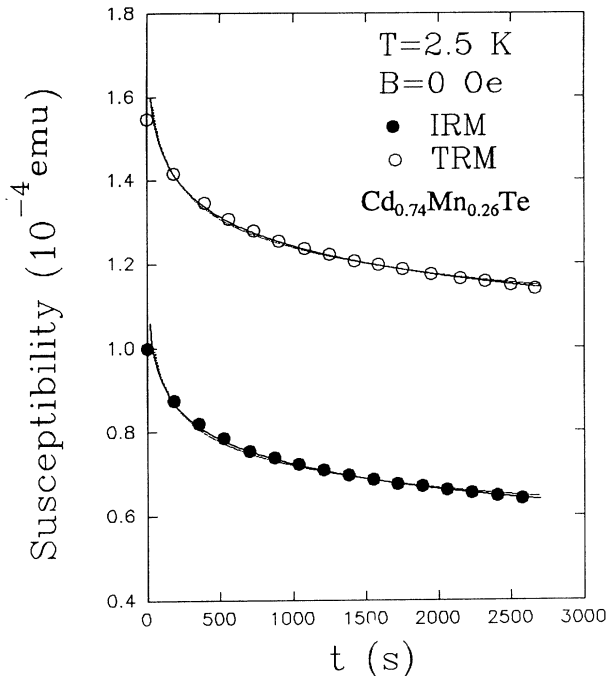


FIG. 2. Relaxation of TRM and IRM of a $\text{Cd}_{0.74}\text{Mn}_{0.26}\text{Te}$ sample measured at zero magnetic field at 2.5 K. The applied magnetic field prior to the relaxation measurements was 1 T. The fitted values of the power-law decay parameter α are 7.76×10^{-2} and 11.13×10^{-2} , for TRM and IRM, respectively. The dotted lines are the least-squares fit of the power-law decay of Eq. (1), and the solid lines are the least-squares fitting of the logarithmic decay of Eq. (2).

at zero magnetic field. The magnetic field applied prior to the relaxation measurements for both cases is 1 T. For IRM, the time duration for 1-T magnetic field application, t_b , is about 5 min. The dotted lines are the least-squares fit of data to a power-law decay,

$$M(t) = M_0 t^{-\alpha} \quad (t > t_0, t_0 \sim 2 \text{ s}), \quad (1)$$

where α is the decay parameter which is directly correlated with the decay rate. The fitted values are $M_0 = 2.12 \times 10^{-4}$, $\alpha = 7.76 \times 10^{-2}$ and $M_0 = 1.55 \times 10^{-4}$, $\alpha = 11.13 \times 10^{-2}$ for TRM and IRM, respectively. Thus both TRM and IRM relaxations can be described here quite well by the power-law decay.

It has been indicated previously that a power-law decay with a small decay parameter α can be fitted reasonably well with a limited time interval by a logarithmic decay¹⁶

$$M(t) = M_0(1 - \alpha \ln t) \quad (t > t_0), \quad (2)$$

which can be obtained from Eq. (1) for small α , i.e., $t^{-\alpha} = e^{-\alpha \ln t} \approx 1 - \alpha \ln t$. The solid lines in Fig. 2 are the least-squares fit of data to Eq. (2) with $t_0 = 2$ s. We see that the logarithmic decay of Eq. (2) fits data equally well as the power-law decay of Eq. (1).

Figure 3 shows the temperature dependence of the decay parameter α of TRM (●) and IRM (○) for a $\text{Cd}_{0.5}\text{Mn}_{0.5}\text{Te}$ sample in the dark. Since we have shown

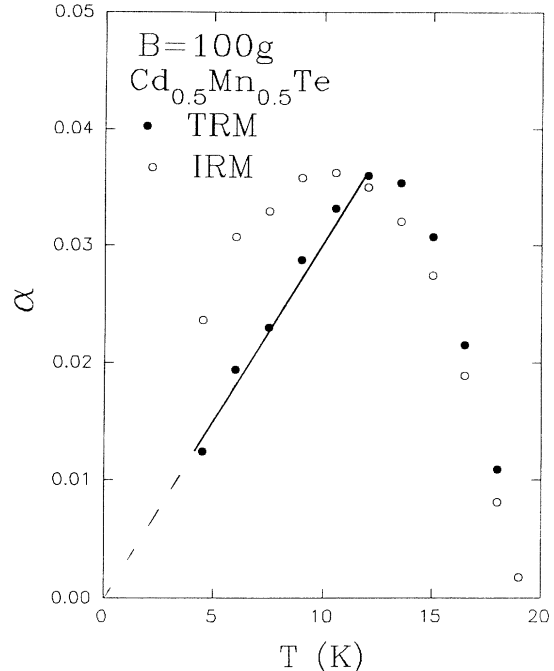


FIG. 3. Temperature dependence of the decay parameter α of TRM (●●●) and IRM (○○○) in the dark for a $\text{Cd}_{0.5}\text{Mn}_{0.5}\text{Te}$ sample. The applied magnetic field was 1 T, and the relaxation data were measured at a reduced magnetic field ($B = 100$ Oe) for both cases. The freezing temperature T_f extrapolated from the data is $T_f = 19$ K for both TRM and IRM. The solid line for TRM indicates the linear relation between α and T from $T = 0$ up to $0.6T_f$.

in Fig. 2 that both power-law and logarithmic decay forms fit data equally well, we present only results obtained from the power-law decay fitting. In the case here, for each temperature, the field applied prior to the relaxation measurements was 1 T for a time duration of about 5 min and the relaxation was measured at a reduced magnetic field ($B = 100$ Oe). Experimental results are different for different time durations of the magnetic-field application, which will be discussed in Fig. 5. For both TRM and IRM, the behaviors are similar. At low temperatures, the power-law decay parameter α increases with increasing temperature, and it depends on temperature almost linearly for TRM up to $0.6T_f$, as indicated by a straight line in Fig. 3, which can be written as $\alpha = aT$. The proportionality constant a obtained from Fig. 3 is $3.1 \times 10^{-3}/\text{K}$. This result is consistent with computer simulation results for SG (Ref. 17) and experimental results for insulating SG.¹⁹ For IRM, we do not have enough data points in the low-temperature region to reach a similar conclusion; however, we expect similar results for IRM in this region. The decay parameter α increases with increasing temperature, and reaches a maximum value of about 0.36 at 10 K for IRM and 12 K for TRM, and then decreases upon further increase of temperature. It approaches zero at a temperature close to the freezing temperature T_f , as we expected. The behavior of α in the high-temperature region for $\text{Cd}_{0.5}\text{Mn}_{0.5}\text{Te}$ is very similar to that of $\text{Cd}_{0.74}\text{Mn}_{0.26}\text{Te}$

(see Fig. 8), i.e., α approaches to zero at T_f .

The important result from Fig. 3 is that there will be no relaxation of magnetization either at $T \rightarrow 0$ or $T \geq T_f$. We would like to emphasize a few points here. First, although $\alpha \rightarrow 0$ at either $T \rightarrow 0$ or $T \geq T_f$, the physical origins behind this are very different. At $T \geq T_f$, there is no remanent magnetization, and the system responds to the applied magnetic field instantaneously. However, at $T \rightarrow 0$, for the case of TRM, the system is in the SG state initially and is not in the equilibrium state after the removal or reduction of the magnetic field. The results in Fig. 3 then indicate that there will be no relaxation of magnetization at $T=0$, and the system will remain in some excited nonequilibrium state, which depends on the history of the system. This result is consistent with our understanding of the SG state. During the relaxation process, the system has to overcome many potential barriers in order to approach the equilibrium state. The existence of these potential barriers is also the reason for the nonexponential decay of the magnetization. In each stage of decay, the system has to overcome potential barriers with different heights by thermal fluctuations. At absolute zero temperature, no potential barriers can be overcome by the system and therefore no decay could be observed.

We have also studied relaxation of TRM and IRM at different magnetic fields. The results for IRM in Fig. 4 were obtained by applying a specific magnetic field for 5 min after the temperature had reached 10 K, then measuring magnetization as a function of time at a reduced field ($B=100$ Oe). The experimental results at different conditions were then fitted by the power-law de-

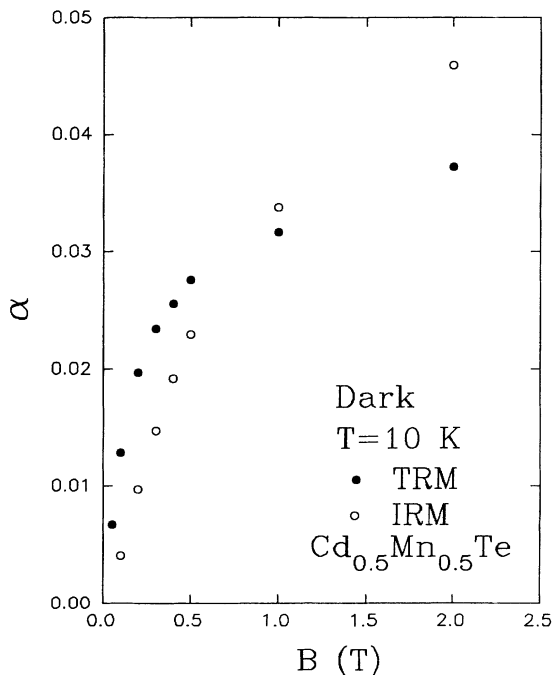


FIG. 4. Applied magnetic-field dependence of the decay parameter α of TRM (●●●) and IRM (○○○) for a $\text{Cd}_{0.5}\text{Mn}_{0.5}\text{Te}$ sample in the dark at $T=10$ K. The time duration for the magnetic-field application was 5 min. Relaxation data were measured at a reduced field of 100 Oe.

decay of Eq. (1). The fitted values of α for different applied magnetic fields are plotted in Fig. 4. There we see that α increases from zero at $B=0$, which is what we expected because remanent magnetization is induced by applying a nonzero magnetic field. The decay parameter α increases rapidly with increasing applied magnetic field in the small field region, and then slowly saturates at a field near 2 T. This behavior is similar to the behavior of the remanent magnetization in insulating SG,¹⁹ and is also in agreement with a Monte Carlo simulation result.¹⁶ Comparing with IRM, α is larger at low magnetic fields for TRM, which probably indicates that its initial state is farther away from the equilibrium. For the case of TRM, the field was on during the cooling down from room temperature. For IRM, on the other hand, the magnetic field was applied at 10 K only for 5 min and so its initial state would be relatively closer to the equilibrium. At higher applied magnetic fields, α becomes larger for IRM, which implies that the situation has been reversed compared to the case at low magnetic fields. This is probably due to the fact that for TRM, the same applied magnetic field affects the system less now because of thermal fluctuation during the cooling down process.

We have also studied how the time duration of an applied magnetic field will affect the relaxation behavior of magnetization. Figure 5 plots the decay parameter α as a function of magnetic field, applying time t_B at two different temperatures, $T=5$ (○) and 10 K (●) for a

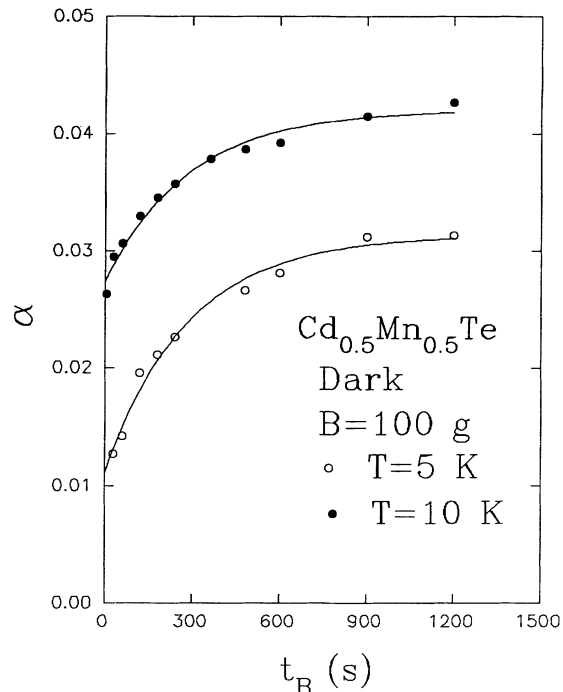


FIG. 5. The dependence of the decay parameter α on the magnetic-field applying time t_B for a $\text{Cd}_{0.5}\text{Mn}_{0.5}\text{Te}$ sample in the dark at two different temperatures $T=5$ (○○○) and 10 K (●●●). The applied and measuring magnetic fields are 1 T and 100 Oe, respectively. The solid lines are the least-squares fit of data using Eq. (3). The fitted values are $\alpha_0=1.1 \times 10^{-22}$, $\alpha_1=2.0 \times 10^{-2}$, and $\tau=2.8 \times 10^2$ s, and $\alpha_0=2.3 \times 10^{-22}$, $\alpha_1=1.5 \times 10^{-2}$, and $\tau=2.4 \times 10^2$ s, for 5 and 10 K, respectively.

$\text{Cd}_{0.5}\text{Mn}_{0.5}\text{Te}$ sample. The applied magnetic field is 1 T, and the measuring field is 100 Oe. There are similarities between the results shown in Figs. 5 and 4, which indicate that applying a higher magnetic field has the same effect on the SG state as applying a lower field for a longer time duration. As we can see from Fig. 5, the decay parameter α increases with increased time duration t_B initially, and then saturates at about 1000 s. The variation of α with t_B is weakly temperature dependent, since the dependence of α on t_B obtained at two different temperatures is almost the same. The solid lines are the least-squares fit of data to the equation,

$$\alpha(t_B) = \alpha_0 + \alpha_1 [1 - \exp(-t_B/\tau)], \quad (3)$$

where α_0 , α_1 , and τ are fitting parameters. The fitted values are $\alpha_0 = 1.1 \times 10^{-2}$ and 2.3×10^{-2} , and $\alpha_1 = 2.0 \times 10^{-2}$, and 1.5×10^{-2} , $\tau = 2.8 \times 10^2$ s, and 2.4×10^2 s for temperatures $T = 5$ and 10 K, respectively.

The results of Fig. 5 show the aging effect. It is expected that for a shorter time duration of a magnetic-field application, the system should be closer to the state before the magnetic-field application due to the freezing properties of SG. So after we have reduced the magnetic field from 1 T to 100 Oe, the magnetization should decay more slowly (small α) because the initial state of the system is closer to the corresponding equilibrium state at 100 Oe. This is exactly what we observed here. The results in Fig. 5 indicate that after turning on the magnetic field, the

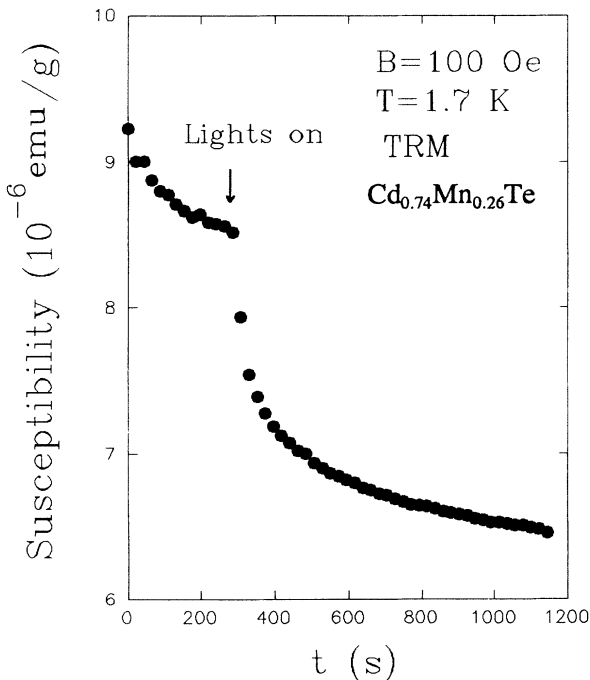


FIG. 6. Decay of magnetic susceptibility of TRM of a $\text{Cd}_{0.74}\text{Mn}_{0.26}\text{Te}$ sample in the dark and under illumination in the spin glass state at $T = 1.7$ K measured at a magnetic field of $B = 100$ Oe. The light excitation source is 100-W white desk lamp with filters. Excitation intensity was about 0.2 W/cm^2 . The arrow indicates the moment the light illumination was turned on. The applied magnetic field during the cooling down was 1 T.

system moves away linearly from the initial state in the phase space. It then approaches a certain region which is relatively fixed in distance from the initial state in the phase space. This process takes for about 1000 s at 1 T.

B. Relaxation under illumination

Figure 6 is the plot of the relaxation of the magnetization for a $\text{Cd}_{0.74}\text{Mn}_{0.26}\text{Te}$ sample at $T = 1.7$ K, and measured at $B = 100$ Oe in the dark and under illumination. Shown in Fig. 6 is an initial decay measured in the dark for about 300 s, and a subsequent decay measured after the moment the light excitation was turned on, as indicated by an arrow in the figure. As we can see from Fig. 6, the decay of the susceptibility under illumination proceeds faster compared to that in the dark.

Figure 7 shows the results of relaxation of magnetization measured at 100 Oe in the dark (●) and under illumination (○) at $T = 1.7$ K for a $\text{Cd}_{0.74}\text{Mn}_{0.26}\text{Te}$ sample together with a power-law decay fitting (solid lines). The experimental results can be described very well by a power law or logarithmic decay both in the dark and under illumination. The fitted values in Fig. 7 are $\alpha = 2.6 \times 10^{-2}$ and 5.4×10^{-2} , and $M_0 = 9.9 \times 10^{-4}$ and 9.4×10^{-4} for the conditions in the dark and under illumination, respectively, which indicates that the decay rate is about a factor of 2 larger under illumination than that in the dark.

Relaxation of the magnetization in $\text{Cd}_{1-x}\text{Mn}_x\text{Te}$ in the SG state has been studied previously. The power-law or logarithmic decay has previously been used to fit ex-

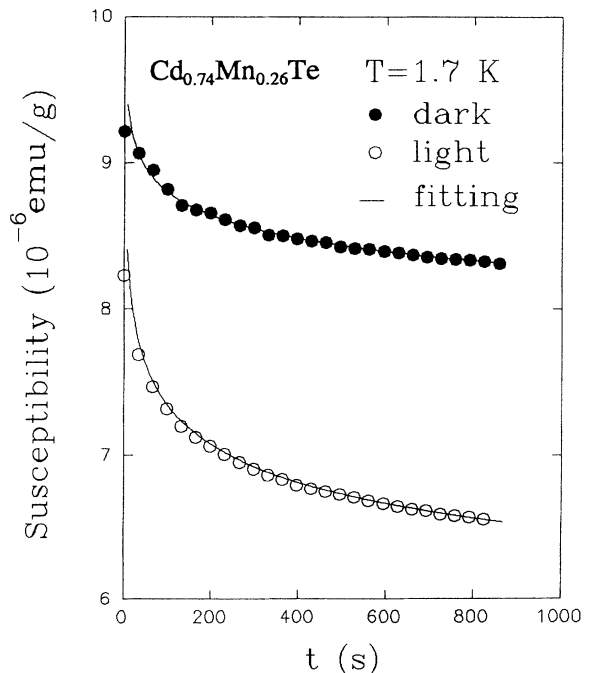


FIG. 7. Decay of magnetic susceptibility of TRM of a $\text{Cd}_{0.74}\text{Mn}_{0.26}\text{Te}$ sample in the dark (●●●) and under illumination (○○○) at $T = 1.7$ K measured at a magnetic field of $B = 100$ Oe. The solid lines are the least-squares fit by the power decay of Eq. (1).

perimental data,^{11,14} which is consistent with our observation here. However, other forms of relaxation, including the stretched exponential decay,²⁰ have also been used to fit SG experimental data. We think that all these forms, including the power-law decay, may just be approximations for the actual decay form under different conditions, which is still not clear at the present. The successful approach for the decay of the remanent magnetization in metallic SG provided a perfect example.²¹ We have also used a stretched-exponential function to fit the decay data and found that the fitting quality is comparable to the power-law decay fitting. However, in performing the temperature and magnetic-field dependencies of magnetization measurements, the fitted decay parameters obtained from the stretched-exponential function scattered, which suggests that the power-law or logarithmic fit is more meaningful. Similar treatments and arguments have been applied previously to the relaxation of persistent photoconductivity in artificially constructed layered materials at low temperatures.²²

Figure 8 plots decay parameter α as a function of temperature in the dark (\circ) and under illumination (\bullet) for $\text{Cd}_{0.74}\text{Mn}_{0.26}\text{Te}$. The decay parameter α decreases linearly with increasing of temperature for both cases. At all temperatures, the magnetization relaxes faster under illumination than in the dark. The difference between α under illumination and in the dark becomes smaller as

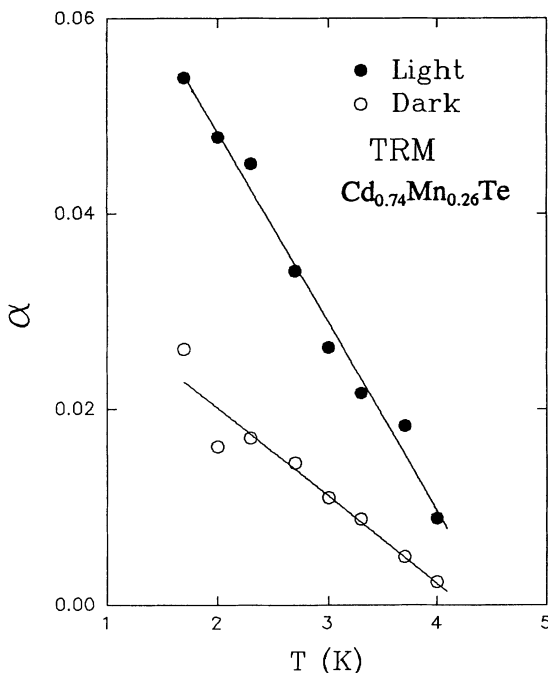


FIG. 8. The decay parameter α as a function of temperature in the dark (\circ) and under illumination (\bullet) for a $\text{Cd}_{0.74}\text{Mn}_{0.26}\text{Te}$ sample. The experimental conditions are the same as those in Fig. 7. The solid lines are the least-squares fit using $\alpha = a - bT$, where a is 3.8×10^{-2} and 8.7×10^{-2} , and b is 9.0×10^{-3} and 1.9×10^{-2} , in the dark and under illumination, respectively. Extrapolate these two lines to $\alpha = 0$ gives $T_f = 4.2 \pm 0.2$ and 4.5 ± 0.2 K for the dark and under illumination.

temperature approaches T_f . Eventually, α approaches zero at the freezing temperature T_f . The dependence of α on temperature T can be described by a linear relation:

$$\alpha = a - bT \quad (T < T_f) . \quad (4)$$

Equation (4) has been used to fit the experimental results as straight lines shown in Fig. 8. The fitted values are $a = 3.8 \times 10^{-2}$ and 8.7×10^{-2} , and $b = 9.0 \times 10^{-3}$ and 1.9×10^{-2} for conditions in the dark and under illumination, respectively. From the fitted values, we find that the temperatures T_f extrapolated from $\alpha = 0$ are 4.2 ± 0.2 and 4.5 ± 0.2 K in the dark and under illumination, respectively, which represent the freezing temperatures. The experimental uncertainty prevents us from concluding whether or not T_f has been changed under illumination.

We have also measured the magnetization of ZFC versus temperature under illumination and in the dark, and still cannot determine whether or not T_f has been changed under illumination, because the difference between the values of T_f in the dark and under illumination is again within experimental uncertainty. However, the values of T_f extrapolated from $\alpha = 0$ in Fig. 8 are consistent with the freezing temperature $T_f (= 4.2 \pm 0.2$ K) obtained from Fig. 1 within the experimental uncertainty. This is what we expected since there will be no remanent magnetization at temperatures above the transition temperature T_f , which is true for cases both in the dark and under illumination. The results in Fig. 8 tell us that we can also determine the freezing temperature T_f of the SG state by measuring the temperature dependence of the relaxation parameters of the magnetization.

In order to see the effects of light excitation on the relaxation of magnetization, or, equivalently, the effects of photogenerated free electrons and holes on the magnetic ion-ion spin interactions in the DMS, we have measured the decay parameter α of TRM at a fixed temperature ($T = 2$ K) under photoexcitation with different light intensities for a $\text{Cd}_{0.74}\text{Mn}_{0.26}\text{Te}$ sample. Figure 9 shows a plot of α versus the square root of excitation light intensity, $I^{1/2}$. In the case here, the magnetic field for the measurements was 100 Oe, and the field applied during the cooling down was 1 T. As we expected, the exponent α increases as light intensity increases. Relaxation of the magnetization obtained under illumination with different light intensities can be described quite well by the power-law or logarithmic decay. The inset of Fig. 9 shows α versus light intensity I . The unit of the light intensity I in the inset is 0.25 W/cm^2 , and that of the square root of intensity $I^{1/2}$ in the main figure is $0.05 \text{ W}^{1/2}/\text{cm}$. The scales of α are the same for both the main figure and the inset. We see that α increases linearly with the square root of light intensity, $\alpha \propto I^{1/2}$.

One obvious possibility which may be responsible for the observed light intensity dependence of α is the heating effect under light excitation. However, the systematic dependence of α on the excitation intensity cannot be explained by considering the heating effects. Furthermore, from Fig. 8 we see that the decay parameter α for $\text{Cd}_{0.74}\text{Mn}_{0.26}\text{Te}$ decreases as the temperature increases in

the temperature region investigated. If the changes of α under light excitation were due to heating, we should expect that α decreases as the light intensity increases, which has never been observed. We have also investigated the intensity dependence of α of TRM and IRM for the $\text{Cd}_{0.5}\text{Mn}_{0.5}\text{Te}$ sample at $T > 12$ K, and a similar behavior is observed. From Fig. 3, for $\text{Cd}_{0.5}\text{Mn}_{0.5}\text{Te}$ at $T > 12$ K, we see again that α should decrease with increasing intensity if the change is due to a heating effect. These observations preclude the possibility of heating effects. Therefore, we can conclude that the decay rate observed to increase under light excitation is due to photoexcited carriers. It is clear from our experimental results that the mechanism responsible for manganese-ion coupling in the DMS is carrier concentration sensitive.

Under photoexcitation, free or localized carriers (electrons and holes) are generated and subsequently recombine radiatively or nonradiatively to emit photons. Photoluminescence due to carrier recombination in DMS's has been observed in many experiments.^{23,24} The electron concentration under illumination can be written as

$$dn/dt = G - Cnp/\tau, \quad (5)$$

where τ is the carrier recombination lifetime, n and p the electron and hole concentrations, and C a proportionality constant in unit of cm^3 . Here G is the carrier generation rate written as

$$G = \alpha_a \eta I / \hbar\omega, \quad (6)$$

with $\hbar\omega$ being the excitation photon energy, I the light intensity in units of W/cm^2 , α_a the absorption coefficient, and η the quantum efficiency—number of electrons generated per each absorbed photon. Under continuous and constant intensity illumination, the photogenerated electrons and holes will be under equilibrium and so we have $dn/dt = 0$. We should also have the condition $n = p$, since our samples are undoped. Then, from Eq. (5), we have

$$n = (G\tau/C)^{1/2} = (\tau\alpha_a\eta/C\hbar\omega)^{1/2} I^{1/2}. \quad (7)$$

From the fact that the relaxation of the magnetization proceeds faster under illumination, we can assume that the relaxation rate of the magnetization is linear in the carrier concentration through the carrier-manganese-ion interactions²⁴ $\alpha \propto n$. From Eq. (7), we have

$$\alpha = B_0 + B_1 I^{1/2}, \quad (8)$$

where B_0 is the decay parameter α in the dark ($I = 0$). In Fig. 9, we have plotted the least-squares fit of data to Eq. (8) as a solid line. The fitted values of B_0 and B_1 obtained from Fig. 9 are 1.57×10^{-2} and 3.68×10^{-3} , respectively.

C. Transient response

We have also measured the transient response of magnetization at different temperatures. Figure 10 shows the susceptibility of $\text{Cd}_{0.5}\text{Mn}_{0.5}\text{Te}$ as a function of time after a 1-T magnetic field was turned on at $T = 6$ K (●), 10 K (□), and 14 K (○). The transient response is a reverse of the relaxation process or remanent magnetization. For relaxation, it takes times for the system to relax from one state to the other. For a transient response, it also takes time for the system to respond to an applied magnetic field. The results shown in Fig. 10 were obtained under the ZFC condition. Here $t = 0$ corresponds to the moment the magnetic field was turned on. We did not observe this slow transient response behavior above T_f . Above T_f , susceptibility saturates instantaneously as soon as the magnetic field is turned on and is a constant independent of magnetic-field applying time. From Fig. 10, we see that below T_f the susceptibility increases with the increase of the magnetic-field applying time. For a clear presentation, the experimental data of Fig. 10 have been subtracted from the susceptibility at $t = 0$, $s(t) = S(t) - S(0)$, where $S(0)$ is the susceptibility at $t = 0$. So Fig. 10 really shows the change of susceptibility as a function of the magnetic-field applying time.

The solid lines in Fig. 10 are the least-squares fit of data with a power-law time dependence,

$$s(t) = s_1 t^\beta \quad (t \geq 0, \beta > 0), \quad (9)$$

where s_1 is a prefactor, and β the transient parameter. We can see that experimental data can be fitted by Eq. (9) very well. We have also tried to use the logarithmic time dependence to describe the transient response. However, the fit is much poorer than those obtained from Eq. (9). This shows that both the transient response and the re-

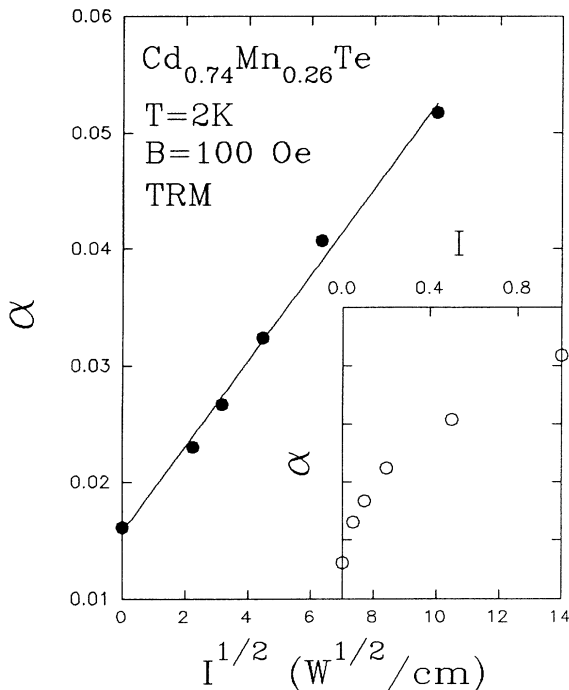


FIG. 9. The dependence of the decay parameter α of TRM on the square root of excitation intensity $I^{1/2}$ for a $\text{Cd}_{0.74}\text{Mn}_{0.26}\text{Te}$ sample at $T = 2$ K. Here $I = 0$ corresponds to the dark. The solid line in the figure is the linear fit of α with $I^{1/2}$ according to Eq. (8) with fitted values of $B_0 = 1.57 \times 10^{-2}$ and $B_1 = 3.68 \times 10^{-3}$. The inset is the plot of α vs light intensity I . The unit of the light intensity I in the inset is $0.25 \text{ W}/\text{cm}^2$, and that of $I^{1/2}$ in the main figure is $0.05 \text{ W}^{1/2}/\text{cm}$. The scales of α are the same for both the main figure and the inset.

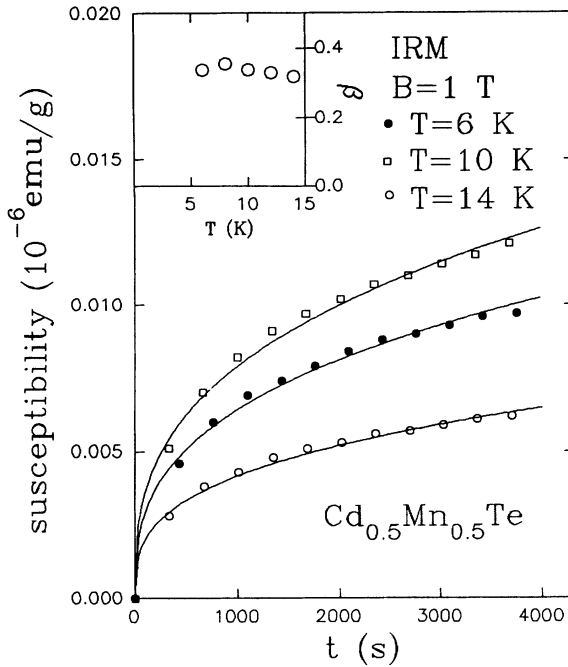


FIG. 10. Transient response of IRM of a $\text{Cd}_{0.5}\text{Mn}_{0.5}\text{Te}$ sample at three different temperatures $T=6$ K (●●●), 10 K (□□□), and 14 K (○○○), measured at a 1-T applied magnetic field. The solid lines are the least-squares fit of data with a power-law time dependence of Eq. (9). The inset shows the temperature dependence of a transient parameter β .

laxation of the magnetization can be described by power-law time dependence. Since the transient response is the reverse of the relaxation process, we would expect that they are strongly correlated.

The inset of Fig. 10 shows the transient parameter β as a function of temperature measured at $B=1$ T. We see that β depends on temperature very weakly in this region. However, the prefactor s_1 depends strongly on temperatures. The values obtained for s_1 are 6.25×10^{-10} , 6.78×10^{-10} , 7.35×10^{-10} , 4.63×10^{-10} , and 4.63×10^{-10} for $T=6, 8, 10, 12,$ and 14 K, respectively.

We have also investigated how the transient response of susceptibility was affected by photoexcitation. Figure 11 shows the susceptibility of $\text{Cd}_{0.5}\text{Mn}_{0.5}\text{Te}$ as a function of time after a 1-T magnetic field was turned on at 10 K under photoexcitation for three different light intensities $I=I_0$ (\circ), $0.63I_0$ (∇), and 0 (\bullet), where I_0 is 0.25 W/cm^2 . The other conditions are the same as those of Fig. 10. Under continuous illumination, the susceptibility increases more quickly at higher excitation intensities. The solid lines in Fig. 11 are the least-squares fitting using Eq. (9). The data obtained at different intensities can be fitted very well by the power-law time dependence of Eq. (9). This indicates that photogenerated carriers play only a role in changing the relaxation rate of the system from one state to the other, but not the form of the process. The fitted values for s_1 and β are $s_1=2.16 \times 10^{-10}$ and $\beta=0.50$, $s_1=1.28 \times 10^{-10}$ and $\beta=0.55$, and $s_1=7.43 \times 10^{-11}$ and $\beta=0.60$ for $I=I_0, 0.63I_0,$ and 0 ,

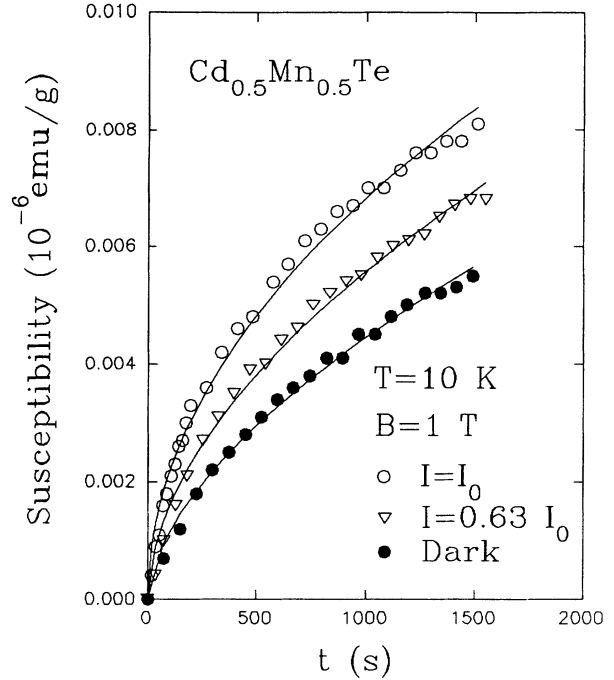


FIG. 11. Transient response of IRM for a $\text{Cd}_{0.5}\text{Mn}_{0.5}\text{Te}$ sample at $T=10$ K under photoexcitation for three different light intensities, $I=I_0$ (\circ), $0.63I_0$ (∇), and 0 (\bullet), where $I_0=0.25 \text{ W/cm}^2$. The applied magnetic field is 1 T. The solid lines are the least-squares fit using Eq. (9) with fitted values of $s_1=2.16 \times 10^{-10}$, 1.28×10^{-10} , and 7.43×10^{-11} , and $\beta=0.50, 0.55,$ and 0.60 , for $I=I_0, 0.63I_0,$ and 0 , respectively.

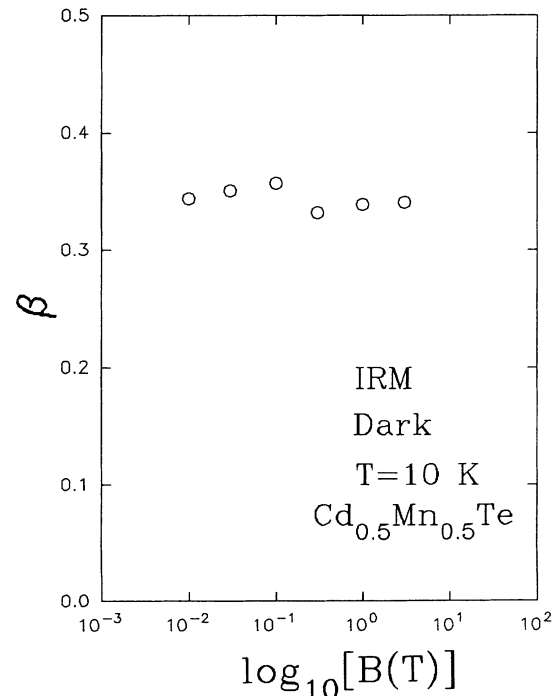


FIG. 12. Applied magnetic-field dependence of β of IRM for a $\text{Cd}_{0.5}\text{Mn}_{0.5}\text{Te}$ sample at $T=10$ K in the dark.

respectively. The parameter s_1 (β) decreases (increases) monotonically with decreasing light intensity I . The increase of β under illumination can be understood in terms of the system becoming relatively easier to change from one state to the other under the presence of photogenerated carriers, similar to the decay process of magnetization. The dependence of s_1 on light intensity I is not clear at this stage.

We have also measured the transient response of magnetization under different magnetic fields. Experimental data at different magnetic fields can be fitted very well by Eq. (9). Figure 12 shows the fitted values of β as a function of applied magnetic field for IRM at $T=10$ K for $\text{Cd}_{0.5}\text{Mn}_{0.5}\text{Te}$. Within three orders of magnetic field, β is almost a constant independent of magnetic field. The parameter $\beta \sim \frac{1}{3}$ shown in both Figs. 12 and 10 may have some significance. It may be correlated with the percolation mechanism of domains in the SG state responding to the applied magnetic field.

D. Discussions

In the following, the mechanisms for the magnetization relaxation at different conditions will be discussed. First, we shall address the aspect of the relaxation rate increasing under light illumination. There are several possible mechanisms which may be responsible for such an effect: (1) the increase of free-carrier and localized magnetic moment interactions due to either superexchange or Ruderman-Kittler-Kasuya-Yosida (RKKY) interaction;²⁴⁻²⁶ (2) light-induced bound magnetic polarons (BMP);²⁷ and (3) modification of spin domains in SG under illumination. RKKY interaction is most important for SG with noble metals (Au, Ag, Cu, Pt) weakly diluted with transition-metal ions, such as Fe or Mn. In these systems, the free-carrier concentration is usually on the order of $10^{21}/\text{cm}^3$. In our case for $\text{Cd}_{1-x}\text{Mn}_x\text{Te}$, the dark carrier concentration is very low since the samples being undoped and the photoexcited carrier concentration is estimated to be on the order of $10^{15}/\text{cm}^3$. Thus we do not expect a significant change of magnetization relaxation due to RKKY interaction at such a low carrier concentration. Also, we did not observe the oscillating character of RKKY interaction while varying the carrier concentration. On the other hand, an increase of magnetic ion-ion spin interaction under illumination cannot explain our results either. The ratio of photogenerated carrier to Mn ions in the sample is less than 1 ppm. Thus the average spin-spin interaction will only be changed by about 10^{-6} , which is not enough to account for the amount of the decay parameter change observed. Light-induced BMP show the influence of the impurity bound carrier on magnetic properties of a system. However, our samples are undoped. Furthermore, photoluminescence data also indicate that the impurity concentration is very low. Therefore, we believe that what we observed is due either to the presence of free carriers or carriers localized by alloy disorder.

Following the above discussion, we think that the most likely mechanism which can account for the experimental results is the modification of domains in SG under il-

lumination. Photogenerated carriers can link different domains via carrier-magnetic ion spin interactions, which will change the domain size distribution and thus the relaxation rate. Recently, Chamberling and Haines²¹ proposed a percolation model for magnetic relaxation in random systems. The model used the activated relaxation of dispersive excitation on a percolation distribution of finite-sized domains, and agreed very well with experimental results. Under this model, the relaxation of magnetization becomes

$$M(t) = M_i \int_0^\infty x^{10/9} \exp(-x^{2/3}) \exp(-tW_- e^{-C/x}) dx, \quad (10)$$

where C is a parameter which describes the relative competition between the average interaction between spins and thermal fluctuation kT , and W_- is the relaxation rate for the largest finite domain. The net relaxation from the percolation model described by Eq. (10) can be derived by assuming (a) relaxation of the magnetization has a linear response among different domains; (b) a given spin is correlated with at least one of its neighbors with probability p , which is determined by the percolation theory; and (c) the relaxation rate is thermally activated with temperature T . Equation (10) becomes a simple power law for $CW_-t \gg 1$, where the power law-decay parameter α depends on C and W_- . In this model, smaller domains have larger energy-level spacing, and relax more slowly than larger ones.

We used Eq. (10) to fit the data for magnetization re-

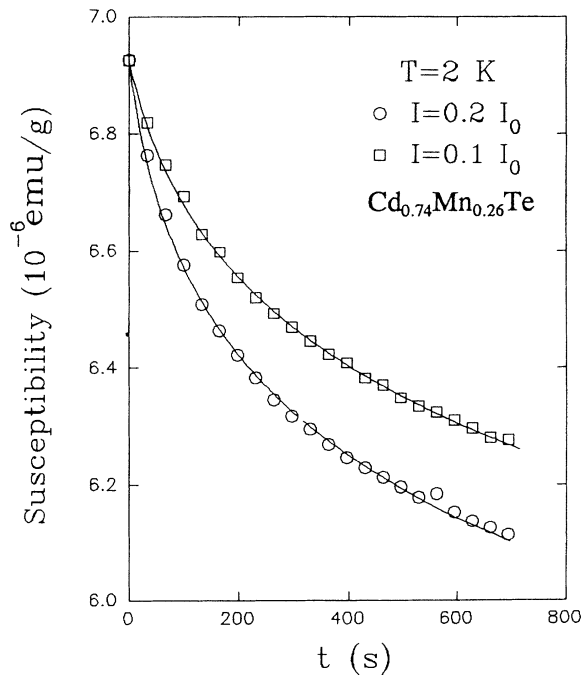


FIG. 13. Relaxation of the magnetic susceptibility of a $\text{Cd}_{0.74}\text{Mn}_{0.26}\text{Te}$ sample under illumination for two representative light intensities $I=0.2I_0$ ($\circ\circ\circ$) and $0.1I_0$ ($\square\square\square$). Experimental data have been used to fit the power-law decay parameter α as shown in Fig. 9. The solid lines are the least-squares fit of data using Eq. (10).

laxation under different conditions. We found that Eq. (10) describes the relaxation in DMS's very well. The experimental results obtained under illumination for two representative excitation intensities for $\text{Cd}_{0.74}\text{Mn}_{0.26}\text{Te}$ are shown in Fig. 13. The solid lines are the least-squares fit using Eq. (10). There are only two adjustable parameters W_- and C for the least-squares fitting. M_i has been fixed from the initial response,²¹ $M_i = (1/3.518)M(0)$. The fitted values of W_- and C as functions of the square root of the light intensity, $I^{1/2}$, are plotted in Fig. 14, where the unit of $I^{1/2}$ is the same as that of Fig. 9. We can see that C depends weakly on the light intensity, which is consistent with our claim that the increase of the relaxation rate is due neither to heating nor enhancement of the average spin-spin interactions. However, W_- increases exponentially with $I^{1/2}$ or carrier concentration n , as shown as a straight line in Fig. 14(a). Since W_- is determined by the largest finite domain in this model, which indicates that photogenerated carriers play the role in affecting the domain size distribution. A natural explanation is that these carriers link different domains which were separated in the dark, resulting in an increase of the domain size. As the photoexcited carrier concentration increases, the largest finite domain size, as well as W_- , increases. The weak dependence on light intensity of C as shown in Fig. 14(b) indicates that the average interaction did not change too much under light illumination.

We have also analyzed experimental data for the aging effects and applied field dependence of the magnetization relaxation by the same model of Eq. (10), which also fitted the data very well. Figure 15 plots fitted values of

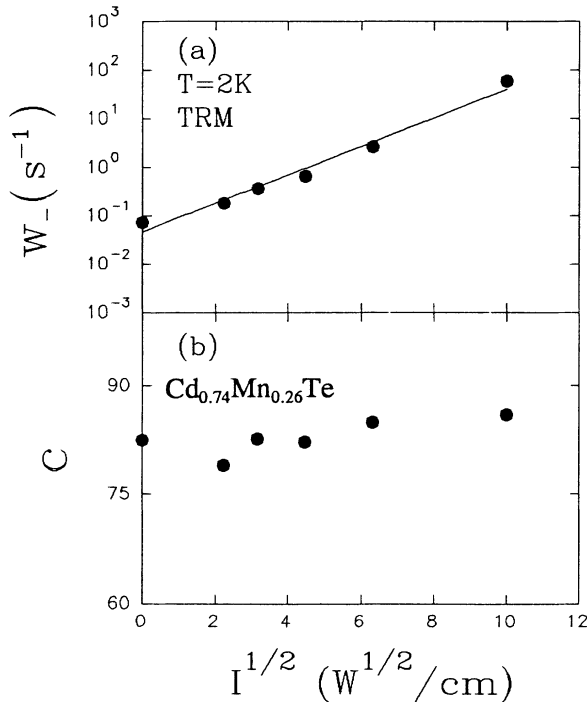


FIG. 14. Plots of fitted values (a) W_- and (b) C as functions of the square root of the light intensity, $I^{1/2}$. The straight line in (a) indicates the exponential increase of W_- with $I^{1/2}$. The scale of $I^{1/2}$ here is the same as that of Fig. 9.

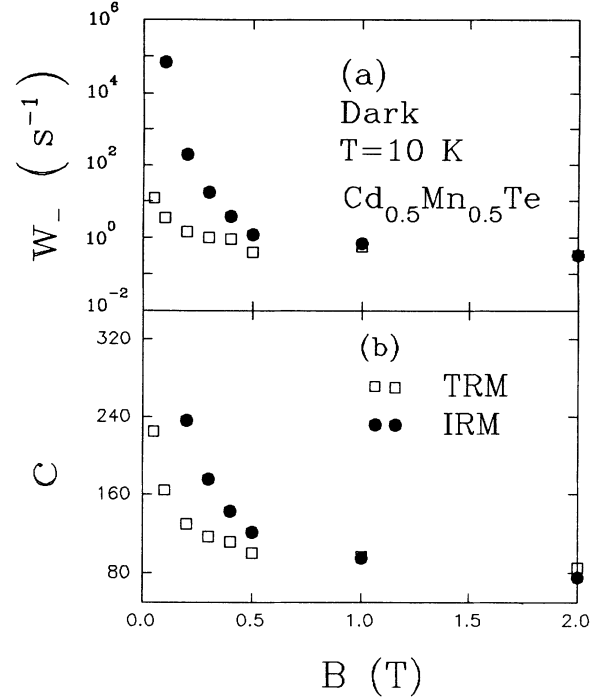


FIG. 15. Plots of fitted values of (a) W_- and (b) C as functions of applied magnetic field. Experimental data are the same as those used to fit the power-law decay parameter α as shown in Fig. 4.

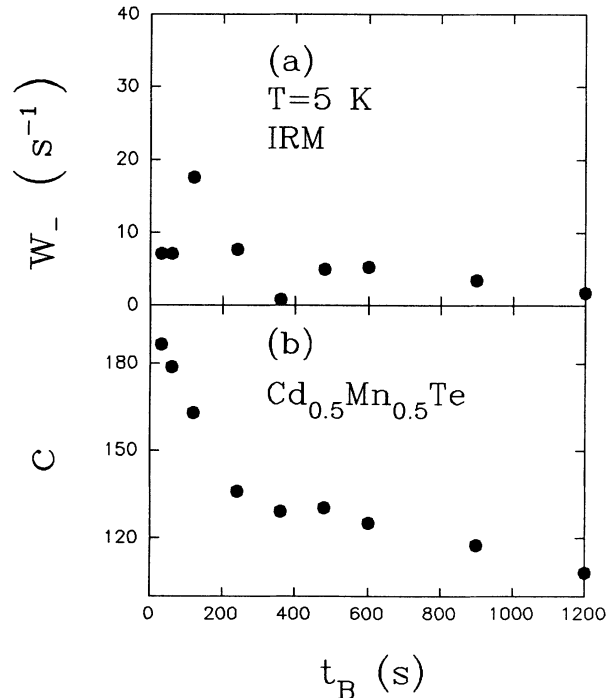


FIG. 16. Plots of fitted values of (a) W_- and (b) C as functions of the magnetic-field applying time t_B . The data are the same as those being used to fit the power-law decay parameter α as shown in Fig. 5.

(a) W_- and (b) C as functions of applied magnetic field B . Experimental data used here are the same as those which were used to obtain the power-law decay parameter α of Eq. (1) shown in Fig. 4. From Fig. 15, both C and W_- decrease as the applied magnetic field increases. This can be understood by recognizing that the spin-spin interaction of Mn ions in DMS's is antiferromagnetic. When an external magnetic field is applied, the number of spins aligned parallel to the direction of the magnetic field increases. As a consequence, the nearest-neighbor spins of Mn ions which paired or clustered with antiparallel alignment will decrease as the applied magnetic field increases. This will reduce the average spin-spin interaction as well as the constant C . This field effect can result in a reduction of the domain size, which shows up as a decrease in W_- .

Figure 16 plots (a) W_- and (b) C as functions of the magnetic-field applying time t_B . The data used here are the same as those which were used to fit the power-law decay parameters α shown in Fig. 5. Similarly, as t_B increases, more spins will be aligned in the field direction. This will decrease the average spin-spin interaction. The same reasoning can be applied to the decrease of C as t_B increases. Since the power-law decay parameter α is inversely proportional to C (under the condition of $CW_-t \gg 1$),²¹ the results shown in Figs. 15 and 16 are consistent with those shown in Figs. 4 and 5. Equation (10) can be applied to both samples for cases either in the dark or under illumination. We show only the results for one of the samples ($x=0.25$) under illumination as representative, similar behaviors have been observed for $x=0.5$. Similarly, the representative results of the aging

effects and the applied field dependence is reported only for $x=0.5$ sample. Thus the percolation model provides a reasonable explanation for our experimental results reported here.

IV. CONCLUSIONS

In conclusion, we have studied the relaxation and transient response of TRM and IRM of SG in $Cd_{1-x}Mn_xTe$ DMS's. Effects of carriers, which are generated by photoexcitation, on the relaxation of TRM and IRM have been studied. A power-law or logarithmic decay for both TRM and IRM, in the dark and under illumination, has been observed. The decay parameter has been measured at different conditions, including temperature, applied magnetic field, and under different intensities of light illumination. We found that the freezing temperature T_f of the SG state can be extrapolated from the temperature dependence of the decay parameter, and that the decay parameter under illumination increases linearly with the photogenerated carrier concentration. The aging effects of TRM and IRM have also been studied. A percolation model, involving an increased spin domain size under illumination due to free-carrier-magnetic ion spin interaction, is used to explain our results.

ACKNOWLEDGMENTS

We acknowledge many helpful discussions with J. Y. Lin, G. Wysin, M. O'Shea, and C. Sorensen. This work was supported by the National Science Foundation under Grants Nos. DMR 91-18818 and OSR 92-55223.

¹*Semiconductors and Semimetals*, edited by J. K. Furdyna and J. Kossut (Academic, New York, 1988), Vol. 25.

²*Diluted Magnetic Semiconductors*, edited by M. Jain (World Scientific, New Jersey, 1991).

³J. Spalek, A. Lewicki, Z. Tarnawski, J. K. Furdyna, R. R. Galazak, and Z. Obuszko, *Phys. Rev. B* **33**, 3407 (1986).

⁴P. Becla, *J. Vac. Sci. Technol. A* **4**, 2014 (1986).

⁵B. S. Sundersheshu, *Phys. Status Solidi A* **61**, K155 (1980).

⁶T. Matsuoka, J. Kuwata, M. Nishikawa, Y. Fujita, T. Tohda, and A. Abe, *Jpn. J. Appl. Phys.* **27**, 592 (1988).

⁷A. K. Ramdas and S. Rodriguez, in *Semiconductor and Semimetals* (Ref. 1), pp. 345-412.

⁸N. Samarth and J. K. Furdyna, *Proc. IEEE* **78**, 990 (1990).

⁹S. Oseroff and P. H. Keesom, in *Semiconductor and Semimetals* (Ref. 1), pp. 73-123.

¹⁰R. R. Galazka, S. Nagata, and P. H. Keesom, *Phys. Rev. B* **22**, 3344 (1980).

¹¹S. B. Oseroff, *Phys. Rev. B* **25**, 6584 (1982).

¹²B. E. Larson, K. C. Hass, and H. Ehrenreich, *Solid State Commun.* **56**, 347 (1985).

¹³C. Domb and N. W. Dalton, *Proc. Phys. Soc. London* **89**, 859 (1966).

¹⁴S. B. Oseroff and F. Gandra, *J. Appl. Phys.* **57**, 3421 (1985).

¹⁵M. Escorne and A. Mauger, *Phys. Rev. B* **25**, 4674 (1982).

¹⁶W. Kinzel, *Phys. Rev. B* **19**, 4595 (1979).

¹⁷C. Dasgupta, S. Ma, and C. Hu, *Phys. Rev. B* **20**, 3837 (1979).

¹⁸M. A. Novak, O. G. Symko, D. J. Zheng, and S. Oseroff, *Physica* **126B**, 469 (1984).

¹⁹J. Ferre, J. Rajchenbach, and H. Maletta, *J. Appl. Phys.* **52**, 1697 (1981).

²⁰M. Ayadi, J. Ferre, A. Mauger, and R. Triboulet, *Phys. Rev. Lett.* **57**, 1165 (1986).

²¹R. V. Chamberlin and Haines, *Phys. Rev. Lett.* **65**, 2197 (1990).

²²H. J. Queisser, *Phys. Rev. Lett.* **54**, 234 (1985).

²³A. Golnik, J. Ginter, and J. A. Gej, *J. Phys. C* **16**, 6073 (1983).

²⁴K. H. Fisher and J. A. Hertz, *Spin Glasses* (Cambridge University Press, New York, 1991).

²⁵W. M. Becker, in *Semiconductor and Semimetals* (Ref. 1), pp. 35-72.

²⁶K. Binder and A. P. Young, *Rev. Mod. Phys.* **58**, 801 (1986).

²⁷T. Wojtowicz, S. Kolesnik, I. Miotkowski, and J. K. Furdyna, *Phys. Rev. Lett.* **70**, 2317 (1993).